European Journal of Mechanics / B Fluids 67 (2018) 220–230

Contents lists available at ScienceDirect

European Journal of Mechanics / B Fluids

journal homepage: www.elsevier.com/locate/ejmflu

Plane blast wave propagation in air with a transverse thermal inhomogeneity

S. Sembian, M. Liverts, N. Apazidis [*]

Department of Mechanics, KTH Royal Institute of Technology, Sweden

ARTICLE INFO

Article history:
Received 19 June 2017
Received in revised form 8 September 2017
Accepted 13 September 2017
Available online 23 September 2017

Keywords:
Thermal inhomogeneity
Shock curvature
Shock broadening/splitting
Exploding wire

ABSTRACT

An alternate mechanism explaining the shock broadening and splitting effects observed during its propagation through an elongated region with transverse thermal inhomogeneity is described. The shock wave is generated by exploding wire technique and its propagation is captured optically using shadowgraph method. Visualizing the flow provided distinct advantage not only for obtaining detailed information on the propagation characteristics but also for validating the numerical scheme used in the analysis. Three physical features namely shock jump, precursor region and vorticity induced flow, are identified to contribute to the shock structure with the latter two being responsible for the pressure profile 'broadening'. The physical behavior of the incident shock is also analyzed along with other factors like temperature and curvature effects.

1. Introduction

The propagation of a shock wave through thermally inhomogeneous media results in shock acceleration in the higher temperature region and consequent shock broadening and splitting. Early experiments [1–19] sparked numerous opinions to explain the fundamental mechanism(s) that cause these effects exhibited by the shock wave. Since those experiments were conducted in weakly ionized plasma, some researchers were inclined towards the inherent plasma-specific phenomena. For example, Klimov et al. [1] reported that the measured velocity of the shock front in the plasma was higher than the calculated velocity in a thermal inhomogeneity and concluded that releasing the energy stored in the vibrational degree of freedom was causing the shock acceleration. They also proposed that the energy of the electron–ion recombination and the energy of the association of atoms into molecules may be released in this region. Gorshkov et al. [2] reported that the measured velocity of the shock front reduced in the presence of a transverse magnetic field further supporting the plasma-specific mechanism. Refs. [8–10] studied the effect of plasma polarity on shock propagation and reported that the formation of a traveling strong double layer near the shock front leads to local electron heating, excitation, ionization and local gas heating with the latter being responsible for shock front broadening and velocity changes in addition to the effect of overall discharge heating.

Adamovich et al. [15] found that there was not enough energy stored because of the low ionization fraction in the discharges and concluded that such effects could hardly be explained by the plasma-specific mechanism. Aithal and Subramanium [17] reported that wall shear could also result in a 'split' signal provided that the shock is very weak (Mach number < 1.025) and propagates longer distances. On the basis of detailed experimental and numerical data [7,9,17,19], it was found that the plasma effects have a thermal nature and can be attributed to the longitudinal and transverse temperature gradients. They emphasized that the fundamental mechanism depends on the transverse temperature gradients resulting in a multi-dimensional nature of shock i.e curved shock and the shock curvature was misinterpreted as 'broadened' and 'split' one-dimensional structure in previous experiments. Therefore they concluded that the main mechanism behind the effects was the shock curvature resulting from spatial inhomogeneity of temperature.

The reported experimental setups at most were fairly similar to one another. Shock waves were produced by a spark discharge resulting in a blast shaped profile. Plasma, either continuous or pulsed, was generated by applying a large potential difference across two ring electrodes housed in a discharge tube. Table 1 summarizes the size of the discharge tube and electrode diameter of some of the facilities.

Laser schlieren method [20] was employed for detecting the shock wave front in Refs. [8–13,15,16,19]. The 'split' schlieren signals were recorded using this method. Macheret et al. [7] measured the temperature profile of the discharge using ultraviolet filtered Rayleigh scattering. The profile was fitted with a gaussian curve with the steady-state centerline temperature varying from 440–830 K (±8%) to a wall temperature of 300 K, ideally filling the entire tube with a transverse temperature gradient. White and

---

[*] Corresponding author.
E-mail address: nap@mech.kth.se (N. Apazidis).

http://dx.doi.org/10.1016/j.euromechflu.2017.09.011

Table 1
Discharge tube size and electrode diameter of some of the reported facilities.

	Tube material	Tube cross-sectional dimension [mm]	Electrode diameter [mm]
Klimov et al. [1]	Plastic	100 × 100	10–60
Gorshkov et al. [2]	Quartz	ϕ 35	30
Ganguly et al. [3–6]	Pyrex	ϕ 50	30
Princeton [7,8]	Quartz	ϕ 38	2–25
White et al. [9]	Pyrex	ϕ 50	25

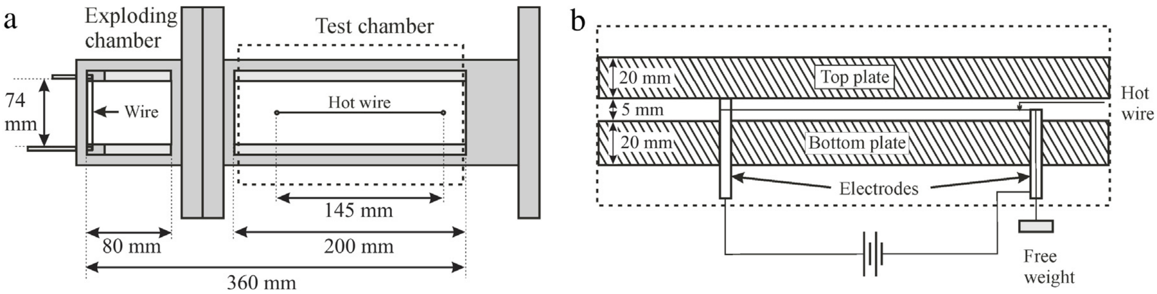

Fig. 1. (a) Test unit (top view). (b) Cut section view of the test chamber (side view).

Subramaniam [9] also measured the centerline temperature and found it to be 1009 K. The experimental error in their temperature measurements was 20%. However, depending on the discharge strength and the ratio between the electrode diameter to the tube inner diameter, there is a probability for existence of a cold gas region near the walls. For instance, Klimov et al. [1] used electrodes with diameters 10–60 mm to produce plasma in a 100 × 100 mm channel. Although no temperature profile measurements were made, the centerline temperature was reported to not exceed 1000 K. Evidently, with the smallest electrode diameter, there is a high probability for the hot region (plasma) to be surrounded by an unaffected cold gas region. In addition, to the knowledge of the authors, the oscilloscope traces from the piezoelectric pressure gauge [1] showing the 'broadened' pressure profile has not been reproduced. Also lacking is an experimental image capturing the shock structure in the inhomogeneity to put the discussion to rest.

In this paper, we describe an alternate mechanism, causing similar effect in a special case where the test area consists of a hot transverse gas region embedded in the cold surrounding air. The dynamical characteristics of the leading shock and the post-shock region are investigated combining both experimental and numerical efforts. Since it was shown that the effects have a thermal nature, we employ an alternative way to generate heat on the principle of Joule heating by subjecting a wire to conduct current. In a certain way this also provides an advantage of 'clean' heat generation without additional plasma effect. The shock wave is generated using exploding wire (EW) technique and the flow is visualized using shadowgraph method. Numerical simulations are performed by solving the full set of Navier–Stokes equations to assist in analyzing and understanding the observed flow features.

This paper is organized as follows. In Section 2, we describe the overall experimental setup including the description of heat generation and optical system. Section 3 presents the governing equations solved along with its validation. In Section 4, the results obtained along with other factors affecting it are discussed and finally in Section 5, this work is summarized.

2. Experimental setup

The experiments were conducted in a test cell consisting of two chambers namely, exploding chamber and test chamber. A schematic of the test cell is shown in Fig. 1(a). A uniform channel of length 360 mm, width 74 mm and height 5 mm runs continuously across both chambers. The exploding chamber houses two electrodes across which a 74 mm long, 0.4 mm diameter copper wire is screwed. The electrodes are connected to a 6 µF, 30 kV capacitor via a spark gap. By triggering the spark gap, the capacitor initially charged to 12 kV is rapidly discharged through the connected wire. As a result of high current flowing through the wire, it undergoes rapid Joule heating during which the wire melts and vaporizes. A cylindrical blast wave moving outward of the EW axis is generated during the expansion phase of the vapor column. The cylindrical blast wave is then quickly modified by the narrow confined rectangular body of the test cell into a plane blast wave which propagates into the test chamber. The top and bottom wall of the test chamber are made up of 20 mm thick Plexiglas plates which can provide a maximum field of view of 200 mm in length for visual access.

Fig. 1(b) represents a cut section view of the test chamber. Two conducting rods, solid (anode) and hollow (cathode), of 3 mm diameter are secured in the bottom plate as shown in Fig. 1(b). The anode which is mounted at 200 mm from the wire explosion plane cuts across the entire 5 mm channel height while the cathode is adjusted to half the height of the channel. The electrodes are made up of brass and the distance between them is 145 mm. A 0.2 mm copper wire is wound around the anode on one end while the other end is passed through the hollow cathode and is attached to a freely suspended weight, making the wire continuously tensed. The wire is then subjected to 15 V, 2.8 A current resulting in heating of the wire. This in turn heats the surrounding gas resulting in hot gas concentrated near the wire and cold gas region around it. Note that the 0.4 mm wire in the exploding chamber generates blasts while the 0.2 mm wire in the test chamber generates heat. Hereinafter 'wire' always corresponds to generating heat unless otherwise stated.

The propagation of the shock wave through the inhomogeneity is captured as shadowgraph images by an optical setup as shown in Fig. 2. The light source is a single pulsed, 532 nm Nd:YAG laser with a pulse width of 4–6 ns and pulse energy of 17 mJ. Since this being a single pulsed laser, only one image per test run can be obtained. The beam from the source is expanded horizontally to 180 mm and rendered parallel by a concave (L1) and convex lens (L2) of focal length (f) −6 mm and 1350 mm respectively. It is then redirected vertically to pass through the test chamber and back to the horizontal plane by a set of two mirrors tilted 45°. The image of the shadowgraph plane is then focused on the camera sensor (Nikon D90) by convex lenses L3 ($f = 1350$ mm) and L4 ($f = 100$ mm). The images captured using this setup had a spatial